The Cause of the Collapse of Yeager Airport Extended Runway

A. S. S. Raghuram[1], S.M. ASCE, B. Munwar Basha[2], M. ASCE

[1]Research Scholar, Dept. of Civil Engineering, Indian Institute of Technology Hyderabad, Kandi, Sangareddy, 502285, Telangana, India, Email: raghuram.ammavajjala@gmail.com
[2]Assistant Professor, Dept. of Civil Engineering, Indian Institute of Technology Hyderabad, Kandi, Sangareddy, 502285, Telangana, India, Email: basha@iith.ac.in

ABSTRACT

Yeager Airport was constructed near Charleston, West Virginia, USA in the 1940's on the top of mountainous terrain. The purpose was to create an even site for the runways. The construction comprised of excavating 7 hilltops and filling nearby valleys. The airport was extended the runway to meet safety regulations. The tallest green faced geosynthetic reinforced slope (GRS) was constructed for this purpose. The geosynthetic reinforced structure is 74 meters high having a slope of 1H: 1V. A portion of the mechanically stabilized earth retention structure failed on 12th March 2015 and the spectacular slide has occurred in the Yeager Airport Expansion Runway. The slide occurred in the south side of the slope. In this paper, an outcome of the forensic analysis of an extended runway is presented. The factors of safety against overstressing and pullout failures are calculated for checking internal stability of reinforced soil slope. By using logarithmic spiral failure mechanism, the tensile strength of reinforcement necessary to maintain the stability was calculated. The possible failure mechanisms considered are: tension failure and pullout failure of the reinforcement. The field data of reinforced, retained and bearing soil zones were collected from the published literature. The paper presents noticeable reasons of failure of reinforced soil retaining wall. From the results of the analysis, it was observed that the considered long term design strength of the reinforcement (T_{all}) was more than adequate to resist the tensile failure. The results also revealed that the available length of the reinforcement was adequate to maintain stability against pullout failure.

INTRODUCTION

Steepened slopes with height more than 70 m have the benefit of increasing land usage, whereas the slope inclination is limited by the characteristics of the in situ soil shear strength. Ground improvement techniques using geosynthetics allow for the construction of slopes with steeper inclination than a natural soil slope through tensile reinforcement and geosynthetic/soil interactions. Extensive use of geosynthetics for more than 20 years to reinforce soil slopes all over the world is clearly visible. The better understanding of the mechanical behaviour of geosynthetically reinforced soil (GRS) slopes which are constructed over different types of foundation soils is necessary. This paper presents a history and forensic analysis of a spectacular slide which has occurred in the Yeager Airport Expansion Runway.

HISTORY, CONSTRUCTION AND COLLAPSE OF YEAGER AIRPORT EXTENDED RUNWAY

Yeager Airport, (formerly Kanawha Airport), construction was completed in 1947 which is present in Charleston, West Virginia. To construct a new airport in Charleston, a committee was setup to evaluate the probable site locations. Due to space constraints, the committee was decided to construct the airport on hilltops as shown in **Fig. 1**. The construction of the new airport began in October 1994. In order to get the large flat site for the airport, it required excavating 7 hilltops and filling the surrounded valleys. Finally, earthwork was completed in 1947. Behind the Panama Canal, it was reported as the second largest earth-moving project in the world at that time. The earthwork consisted of moving more than 6,881,000 m^3 of earth and rock. It required more than 907,000 kilograms of explosives for the earthwork. The project cost approximately $4.5 million, which is more than 34 times the cost of the site.

Figure 1. Yeager Airport situated on series of semi-connected hill tops know as "Coonskin Ridge. (Courtesy Google Earth, downloaded on Sep 20, 2016)

Due to the dramatic slopes of 91 m height around the airport, they could not meet with the Federal Aviation Administration (FAA) safety regulations and a few concessions were made. Finally, the airport was completed in 1947 and came into operational on December 01. Moreover, the committee decided to upgrade the Yeager airport facilities in order to meet the FAA safety regulations. For this upgradation to meet FAA safety regulations, Runway 5 required a 150 m extension as the previous runway did not include the emergency stopping area. Lostumbo (2010) reported that reinforced steepened slope was determined to be the best option for the project as it offered an economical solution. In addition, Lostumbo (2010) reported that the construction of the 1:1 reinforced slope was completed in just under 2 years, starting in the late summer of 2005 and finishing in spring 2007. On, 11th Mar 2015, the Charleston Daily Mail reported that six residents were moved out of their houses below the slope as the movement of the slope was detected. On, 12th Mar 2015, this quickly developed into a very large-scale landslide as shown in **Figs. 2, 3** and **4**. Formation of fissures before failure was shown in **Fig. 3(a)** and **3(b)**.

This paper mainly focuses on the collapse of Yeager airport extended runway. In an attempt to recognize probable causes for the collapse, a broad analytical investigation was carried out by computing the internal stability against tensile failure and pullout failure, based on the current design approaches. For the internal stability of GRS structure, safety against tension and pullout failure should be ensured for the satisfactory design. The factors of safety against overstressing and pullout failures are calculated for checking the internal stability of GRS. By using logarithmic spiral failure mechanism as reported by Basha and Babu (2012), the tensile strength of reinforcement necessary to maintain the stability was calculated. The field data of reinforced, retained and bearing soil zones were collected from published literature (Lostumbo 2010). The most likely causes about the collapse of the slope are provided at the end of the paper.

Figure 2. The failure of Yeager airport expansion runway as reported by Charleston Gazette-Mail on 12 Mar 2015
(http://www.wvgazettemail.com/article/20150312/DM05/150319672)

(a) At the base of the slope (b) Close view of the fissures

Figure 3. Formation of fissures at the bottom of the slope
(Source: Geotechpedia blog, March 20, 2015. http://blog.geotechpedia.com/index.php/2015/03/what-could-have-gone-wrong-in-yeager-airport-expansion-slide/)

Subsurface Exploration

As reported by Lostumbo (2010) the site consisted of fill, colluvial and shallow rock. Slope bearing area mainly consisted of weathered sandstone underlain by shale.

Table 1. Geotechnical properties of soil as reported by Lostumbo (2010)

Property	Value
Sand stone and Sand material Maximum Dry Density Optimum Moisture Content	 19.2 to 20.9 kN/m^3 8.3 to 11.8 %
Clay with rock fragments Maximum Dry Density Optimum Moisture Content	 17.9 to 18.8 kN/m^3 12.1 to 12.6 %
Internal friction angle of weathered sandstone	38.9^o to 39.6^o
Compressive strength of weathered sandstone	30,405 to 97,630 kPa

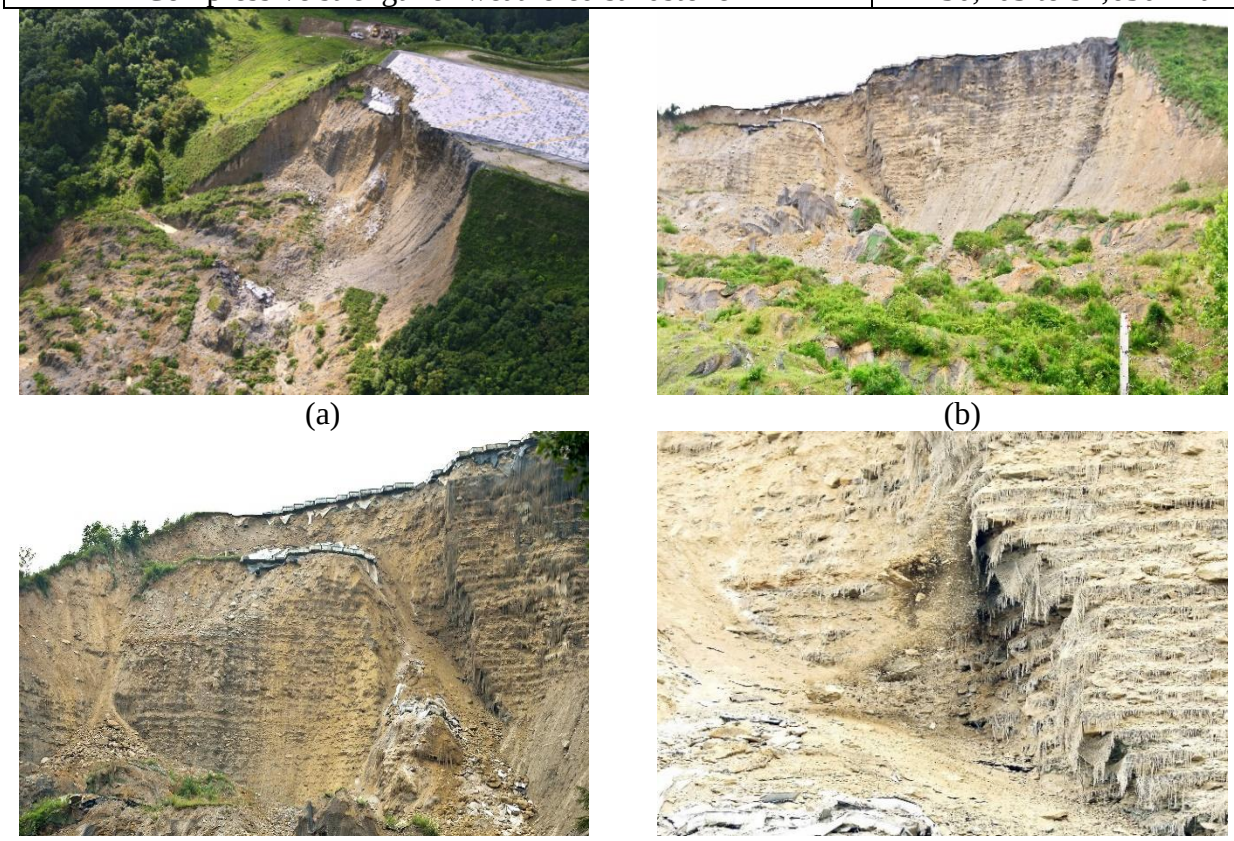

(a) (b) (c) (d)

Figure 4. Collapse of extended runway (a) View from top, (b) Long front view, (c) Close front view, (d) Failure of reinforcement

(Source: (a) Charleston Gazette Mail, Feb 24-2016, http://www.wvgazettemail.com/news/20160224/yeager-chairman-says-rebuilding-collapsed-safety-zone-airports-top-priority , (b), (c), and (d) Charleston Gazette Mail, July 15-2015, http://www.wvgazettemail.com/article/20150715/DM01/150719584/200404251)

Table 1 summarizes the geotechnical properties of the soil.

Design Considerations

The soil properties that are used in the design was categorized into three zones namely reinforced soil, retained soil, and bearing soil zones. The unit weights for the above respective zones are

18.1, 18.1, and 22.0 kN/m^3. The cohesionless is considered for all the three zones. The internal frictional angle varied as 36^o, 36^o, and 40^o respectively for reinforced, retained and bearing soil zones. Three different types of primary and secondary reinforcement of different strengths as provided by Lostumbo (2010) are adopted for the design. The long term design strength (T_{all}) of the reinforcements which are used for the design are provided in **Fig. 5.** The geogrids used were woven polyester uniaxial geogrids coated with PVC. As shown in the Fig. 3, the length of the geogrid varied from 44 m in the top 37 m segment at a spacing of 0.9 m and 53 m in the bottom 37 m of the segment at a spacing of 0.45 m. The minimum ultimate tensile strength of the geogrid reinforcement (T_{ult}) used in the three zones are 160.1, 154.5, and 123.2 kN/m respectively. The actual values of T_{ult} in the three zones are 187.9, 187.9 and 145.2 kN/m respectively. **Fig. 5** clearly shows the arrangement and placement of geogrid layers as reported by Tencate.

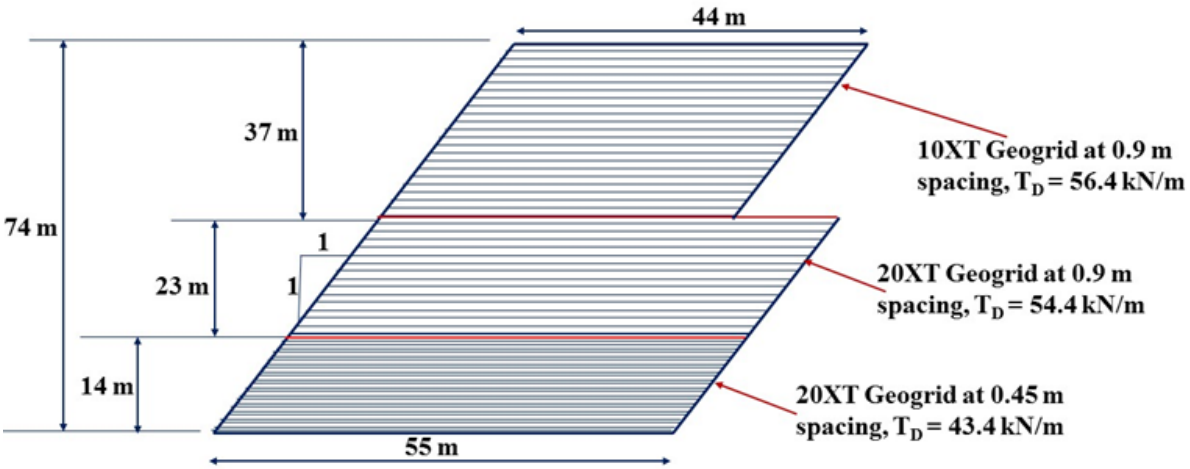

Figure 5. Cross section of Yeager airport extended runway slope (as reported by Tencate).

INTERNAL STABILITY ANALYSIS

Limit equilibrium approach is used as suggested by FHWA (2001). The analysis developed by Basha and Babu (2012) is used to calculate reinforcement force coefficient (K) to stabilize the slope. The factors of safety against tension and pullout failure modes are provided in the following sections.

Factor of Safety against Tension Failure

For the slope to be stable, the main criterion is the maximum load in the reinforcement layers ($T_{i\max}$) should be less than the design tensile strength of the reinforcement layer (T_D). The factor of safety against tension (FS_t) is given by Eq. 1.

$$FS_t = \frac{T_D}{T_{i\max}} \tag{1}$$

where $T_{i\max}$ can be calculated by using the following equation.

$T_{i\max} = (z\gamma + q)K(S_v \times S_h)$

Where S_v = vertical spacing = H/n, S_h = horizontal spacing = 1m, n = number of reinforcement layers and z = depth of layer of reinforcement.

The number of geogrid layers of reinforcement was 98 (i.e. n = 98) as reported by Tencate. As shown in Fig. 3, the spacing of reinforcement in the top 60 m portion is 0.9 m. For the remaining 14 m height of slope, the spacing is 0.45 m.

Factor of Safety against Pullout Failure

For the slope to be stable, the maximum load in the soil reinforcement ($T_{i\max}$) should be less than available resisting force (P_{ri}) on the embedded reinforcement length (L_{ei}) of the layer. The factor of safety against tension (FS_{po}) is given by

$$FS_{po} = \frac{P_{ri}}{T_{i\max}} \qquad (2)$$

where $P_{ri} = 2\sigma_{vi} L_{ei} \tan\delta$, $\sigma_{vi} = z\gamma$ is the effective vertical stress and δ is interface friction angle between soil and reinforcement. The available resisting force P_{ri} depends on embedded length of reinforcement as shown in Fig. 5

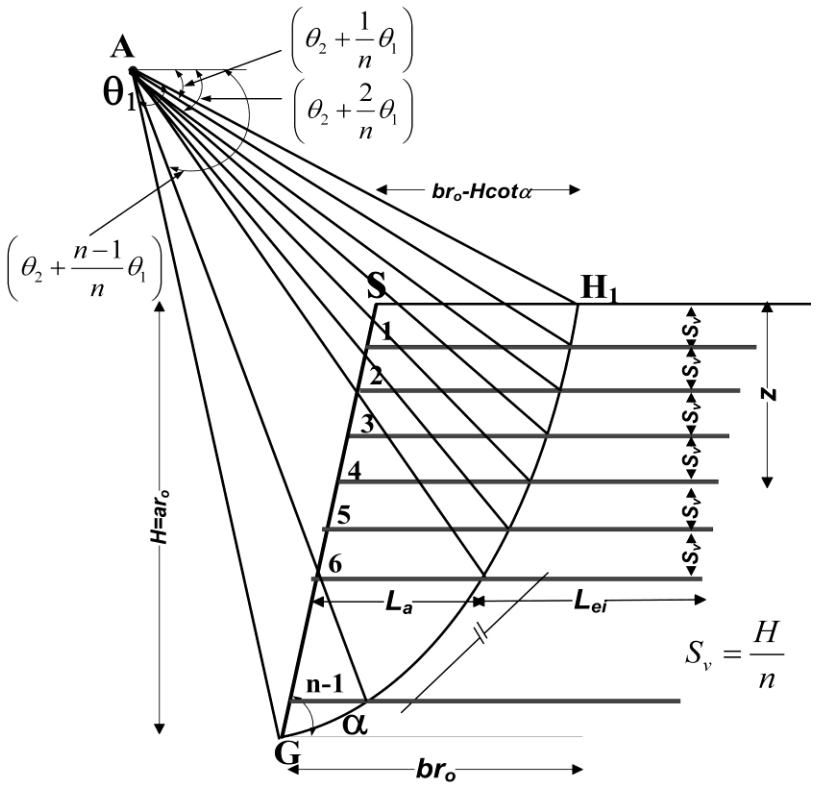

Figure. 6(a) Calculation of L_a and L_t for all layers (Basha and Babu 2012)

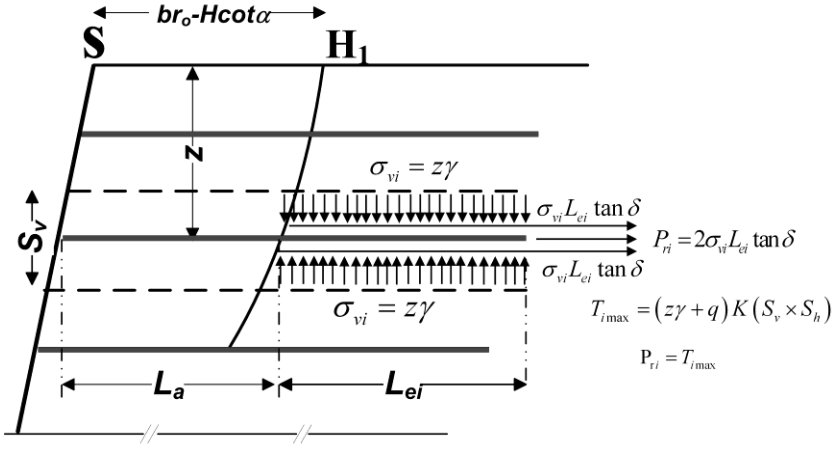

Figure. 6(b) Calculation of pullout length of reinforcement (Basha and Babu 2012)

Estimation of Total Length of Reinforcement

In the analysis logarithmic spiral failure mechanism was used. The total length of reinforcement is divided in to two parts, when the log spiral failure surface passes through the toe of the reinforced wall as shown in **Fig. 6(a)** and **6(b)**. From **Fig. 6(a)** the total length of reinforcement can be written as

$$L_t = L_a + L_{ei} \tag{3}$$

where

$L_a = br_o - L_s - L_b$, $L_s = (H - Z)\cot\alpha$ and $L_b = r_o \cos\theta_2 - r\cos(\theta_2 + \theta)$

The active length of reinforcement (L_a) is obtained by maximizing the reinforcement force coefficient (K) required to stabilize the wall and it can be calculated using.

$$\frac{L_a}{H} = \frac{1}{a}[e^{\theta\tan\phi}\cos(\theta_2 + \theta) - e^{\theta_1\tan\phi}\cos(\theta_1 + \theta_2)] - (1 - \frac{Z}{H})\cot\alpha \tag{4}$$

where $\frac{Z}{H} = \frac{1}{a}[e^{\theta\tan\phi}\sin(\theta_2 + \theta) - \sin\theta_2]$ and $\theta = i(\theta_1 / n)$, i = 1 to n-1

RESULTS AND DISCUSSIONS

Checking Adequacy of Safety against Internal Stability Modes

The results of the stability analysis on the collapsed Yeager Airport extended runway are presented here. The magnitudes of FS_t and FS_{po} are computed for three different reinforcement strengths, γ = 18.1 kN/m^3, K = 0.025 (which is obtained from Basha and Babu, 2012), S_h = 1 m, tanδ = 0.486, α = 0.8, pullout factor = 0.61, ϕ = 36^o and reported in Tables 2(a) and 2(b). It can be noted from **Tables 2(a)** and **2(b)** that magnitude of FS_t with respect to depth decreases due to increase in $T_{i\max}$. Moreover, the magnitude of FS_{po} increases with depth due to increase in P_{ri} value. The increase in P_{ri} is more due to effective overburden pressure. An important observation that can be made from **Tables 2(a)** and **2(b)** that the GRS constructed for extension of Yeager

Airport runway ensures stability against tension and pullout failure modes as both factors of safety are more than 1.5 (recommended by FHWA, 2001) for all 98 layers of reinforcement from top to bottom of the slope. The magnitudes of factors of safety indicate that the reinforced soil slope is overly safe for the values reported by Lostumbo (2010). Therefore, the failure cannot be attributed to the internal stability modes. Now, the cause of collapse may be due to inadequate external stability.

Effect of Reduction in Friction Angle of the Reinforce Soil on Internal Stability

Fig. 8(a) shows the variation of a factor of safety against tension failure (FS_t) of 98 layers of reinforcement along the depth of wall for ϕ = 36°, 34°, 32°, 30°, 28° and 26° and typical values mentioned in the above sections. For the top layers where an axial tensile force in the geosynthetic layer is significantly less, a very high value (i.e. 118.41) of factor of safety is observed. It can be observed from the figure that the bottom layers of reinforcement from the top of the wall are more critical to the tension mode of failure due to overburden pressure and generally have a lower factor of safety values for $\phi \leq$ = 30°. The results presented in **Fig. 8(b)** show the variation of factor of safety against pullout failure (FS_{po}) of 98 layers of reinforcement along the depth of wall for ϕ = 36°, 34°, 32°, 30°, 28° and 26°. It can be noted from **Fig. 8(b)** that the upper layers of reinforcement from the top of the wall are more critical to the pullout mode of failure and slope does not have adequate pullout length to maintain the factor of safety against pullout failure (FS_{po}) more than 1.5 for $\phi \leq$ = 28°.

Table 2(a). Factors of safety against tension and pullout failure modes

Layers No	depth, Z (m)	S_v (m)	$T_{i\max}$ (kN/m)	FS_t	L_a (m)	L_{ei} = (m)	P_{ri} (kN/m)	FS_{po}
1	0.90	0.9	0.37	118.41	15.77	28.23	218.45	595.99
2	1.80	0.9	0.73	59.20	15.68	28.32	438.25	597.84
3	2.70	0.9	1.10	39.47	15.59	28.41	659.43	599.72
4	3.60	0.9	1.47	29.60	15.50	28.50	882.05	601.63
5	4.50	0.9	1.83	23.68	15.41	28.59	1106.12	603.57
6	5.40	0.9	2.20	19.73	15.32	28.68	1331.68	605.54
7	6.30	0.9	2.57	16.92	15.22	28.78	1558.77	607.55
8	7.20	0.9	2.93	14.80	15.12	28.88	1787.42	609.58
9	8.10	0.9	3.30	13.16	15.03	28.97	2017.68	611.65
10	9.00	0.9	3.67	11.84	14.93	29.07	2249.57	613.76
11	9.90	0.9	4.03	10.76	14.83	29.17	2483.12	615.89
12	10.80	0.9	4.40	9.87	14.72	29.28	2718.39	618.05
13	11.70	0.9	4.76	9.11	14.62	29.38	2955.39	620.25
14	12.60	0.9	5.13	8.46	14.51	29.49	3194.17	622.48
15	13.50	0.9	5.50	7.89	14.41	29.59	3434.76	624.74
16	14.40	0.9	5.86	7.40	14.30	29.70	3677.20	627.04
17	15.30	0.9	6.23	6.97	14.19	29.81	3921.53	629.37
18	16.20	0.9	6.60	6.58	14.08	29.92	4167.77	631.72
19	17.10	0.9	6.96	6.23	13.96	30.04	4415.97	634.12
20	18.00	0.9	7.33	5.92	13.85	30.15	4666.16	636.54
21	18.90	0.9	7.70	5.64	13.73	30.27	4918.38	639.00
22	19.80	0.9	8.06	5.38	13.61	30.39	5172.66	641.49

23	20.70	0.9	8.43	5.15	13.49	30.51	5429.04	644.01
24	21.60	0.9	8.80	4.93	13.37	30.63	5687.55	646.56
25	22.50	0.9	9.16	4.74	13.25	30.75	5948.24	649.15
26	23.40	0.9	9.53	4.55	13.13	30.87	6211.13	651.77
27	24.30	0.9	9.90	4.39	13.00	31.00	6476.27	654.42
28	25.20	0.9	10.26	4.23	12.87	31.13	6743.69	657.11
29	26.10	0.9	10.63	4.08	12.74	31.26	7013.43	659.82
30	27.00	0.9	11.00	3.95	12.61	31.39	7285.52	662.58
31	27.90	0.9	11.36	3.82	12.48	31.52	7560.00	665.36
32	28.80	0.9	11.73	3.70	12.35	31.65	7836.90	668.18
33	29.70	0.9	12.10	3.59	12.21	31.79	8116.27	671.03
34	30.60	0.9	12.46	3.48	12.08	31.92	8398.14	673.91
35	31.50	0.9	12.83	3.38	11.94	32.06	8682.55	676.82
36	32.40	0.9	13.19	3.29	11.80	32.20	8969.53	679.77
37	33.30	0.9	13.56	3.20	11.66	32.34	9259.13	682.75
38	34.20	0.9	13.93	3.12	11.51	32.49	9551.37	685.77
39	35.10	0.9	14.29	3.04	11.37	32.63	9846.29	688.82
40	36.00	0.9	14.66	2.96	11.22	32.78	10143.94	691.90
41	36.90	0.9	15.03	2.89	11.08	32.92	10444.35	695.01
42	37.80	0.9	15.39	3.53	10.93	42.07	13672.31	888.16
43	38.70	0.9	15.76	3.45	10.78	42.22	14047.98	891.34
44	39.60	0.9	16.13	3.37	10.62	42.38	14426.52	894.55
45	40.50	0.9	16.49	3.30	10.47	42.53	14807.98	897.80
46	41.40	0.9	16.86	3.23	10.32	42.68	15192.37	901.08
47	42.30	0.9	17.23	3.16	10.16	42.84	15579.76	904.40
48	43.20	0.9	17.59	3.09	10.00	43.00	15970.16	907.75
49	44.10	0.9	17.96	3.03	9.84	43.16	16363.62	911.13

Table 2(b). Factors of safety against tension and pullout failure modes

Layers No	depth, Z (m)	S_v (m)	$T_{i\max}$ (kN/m)	FS_t	L_a (m)	L_{ei} (m)	P_{ri} (kN/m)	FS_{po}
50	45.00	0.90	18.33	2.97	9.68	43.32	16760.17	914.54
51	45.90	0.90	18.69	2.91	9.51	43.49	17159.86	917.99
52	46.80	0.90	19.06	2.85	9.35	43.65	17562.72	921.48
53	47.70	0.90	19.43	2.80	9.18	43.82	17968.79	925.00
54	48.60	0.90	19.79	2.75	9.01	43.99	18378.11	928.55
55	49.50	0.90	20.16	2.70	8.84	44.16	18790.71	932.13
56	50.40	0.90	20.53	2.65	8.67	44.33	19206.64	935.75
57	51.30	0.90	20.89	2.60	8.50	44.50	19625.92	939.40
58	52.20	0.90	21.26	2.56	8.33	44.67	20048.61	943.09
59	53.10	0.90	21.62	2.52	8.15	44.85	20474.73	946.81
60	54.00	0.90	21.99	2.47	7.97	45.03	20904.33	950.56
61	54.90	0.90	22.36	2.43	7.79	45.21	21337.44	954.35
62	55.80	0.90	22.72	2.39	7.61	45.39	21774.11	958.18
63	56.70	0.90	23.09	2.36	7.43	45.57	22214.37	962.03
64	57.60	0.90	23.46	2.32	7.24	45.76	22658.25	965.92
65	58.50	0.90	23.82	2.28	7.06	45.94	23105.81	969.85
66	59.40	0.90	24.19	2.25	6.87	46.13	23557.07	973.81

67	60.30	0.90	24.56	2.22	6.68	46.32	24012.07	977.80
68	60.75	0.45	12.37	4.56	6.49	46.51	24290.93	1963.66
69	61.20	0.45	12.46	4.53	6.30	46.70	24572.12	1971.79
70	61.65	0.45	12.55	4.49	6.10	46.90	24855.66	1979.98
71	62.10	0.45	12.65	4.46	5.91	47.09	25141.57	1988.24
72	62.55	0.45	12.74	4.43	5.71	47.29	25429.88	1996.58
73	63.00	0.45	12.83	4.40	5.51	47.49	25720.61	2004.98
74	63.45	0.45	12.92	4.37	5.31	47.69	26013.76	2013.45
75	63.90	0.45	13.01	4.33	5.11	47.89	26309.37	2021.99
76	64.35	0.45	13.10	4.30	4.91	48.09	26607.46	2030.60
77	64.80	0.45	13.19	4.27	4.70	48.30	26908.03	2039.28
78	65.25	0.45	13.29	4.24	4.49	48.51	27211.12	2048.02
79	65.70	0.45	13.38	4.22	4.28	48.72	27516.75	2056.84
80	66.15	0.45	13.47	4.19	4.07	48.93	27824.92	2065.73
81	66.60	0.45	13.56	4.16	3.86	49.14	28135.67	2074.68
82	67.05	0.45	13.65	4.13	3.65	49.35	28449.02	2083.71
83	67.50	0.45	13.74	4.10	3.43	49.57	28764.98	2092.81
84	67.95	0.45	13.84	4.08	3.21	49.79	29083.58	2101.97
85	68.40	0.45	13.93	4.05	3.00	50.00	29404.83	2111.21
86	68.85	0.45	14.02	4.02	2.78	50.22	29728.76	2120.52
87	69.30	0.45	14.11	4.00	2.55	50.45	30055.38	2129.89
88	69.75	0.45	14.20	3.97	2.33	50.67	30384.72	2139.34
89	70.20	0.45	14.29	3.95	2.10	50.90	30716.80	2148.86
90	70.65	0.45	14.39	3.92	1.88	51.12	31051.63	2158.45
91	71.10	0.45	14.48	3.90	1.65	51.35	31389.25	2168.10
92	71.55	0.45	14.57	3.87	1.42	51.58	31729.66	2177.83
93	72.00	0.45	14.66	3.85	1.19	51.81	32072.89	2187.63
94	72.45	0.45	14.75	3.82	0.95	52.05	32418.96	2197.50
95	72.90	0.45	14.84	3.80	0.72	52.28	32767.89	2207.44
96	73.35	0.45	14.94	3.78	0.48	52.52	33119.70	2217.46
97	73.80	0.45	15.03	3.75	0.24	52.76	33474.41	2227.54
98	74.25	0.2	15.12	3.73	0.00	53.00	33832.05	2237.69

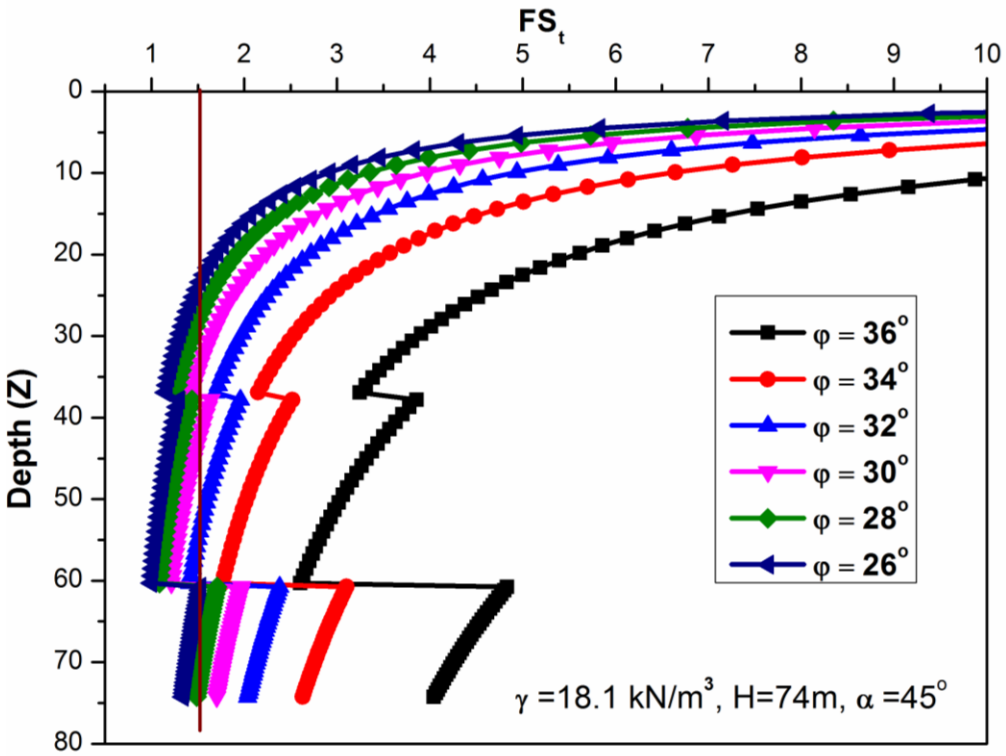

Figure 8(a). Factors of safety against tension failure for different values of ϕ

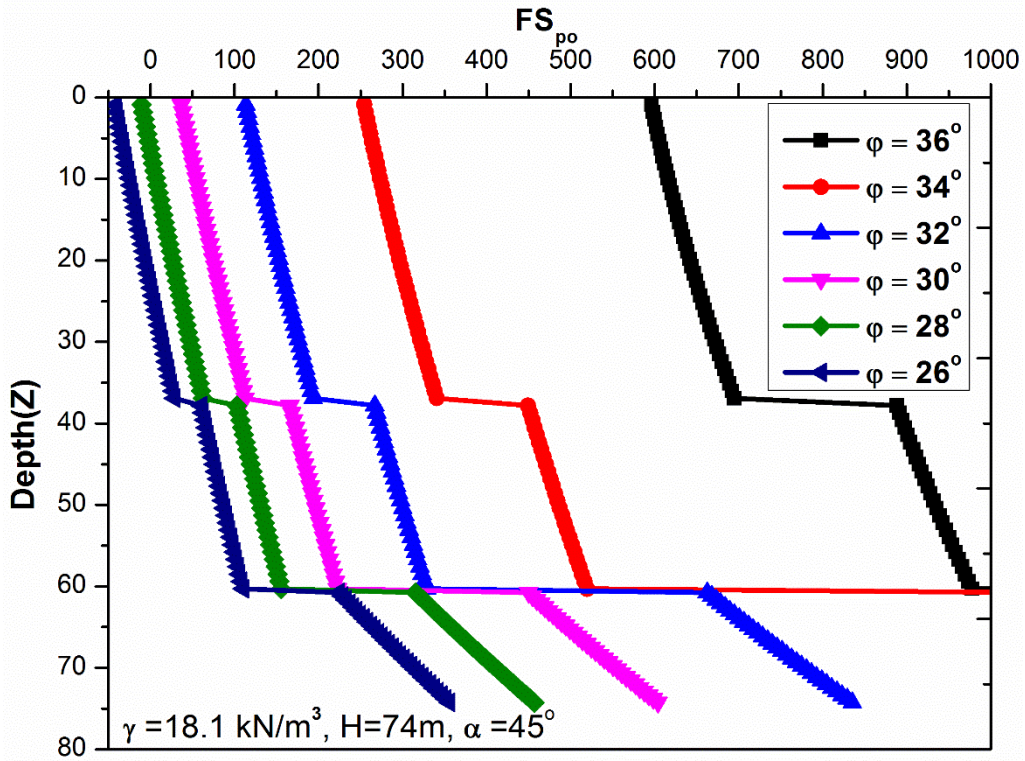

Figure 8(b). Factors of safety against pullout failure for different values of ϕ

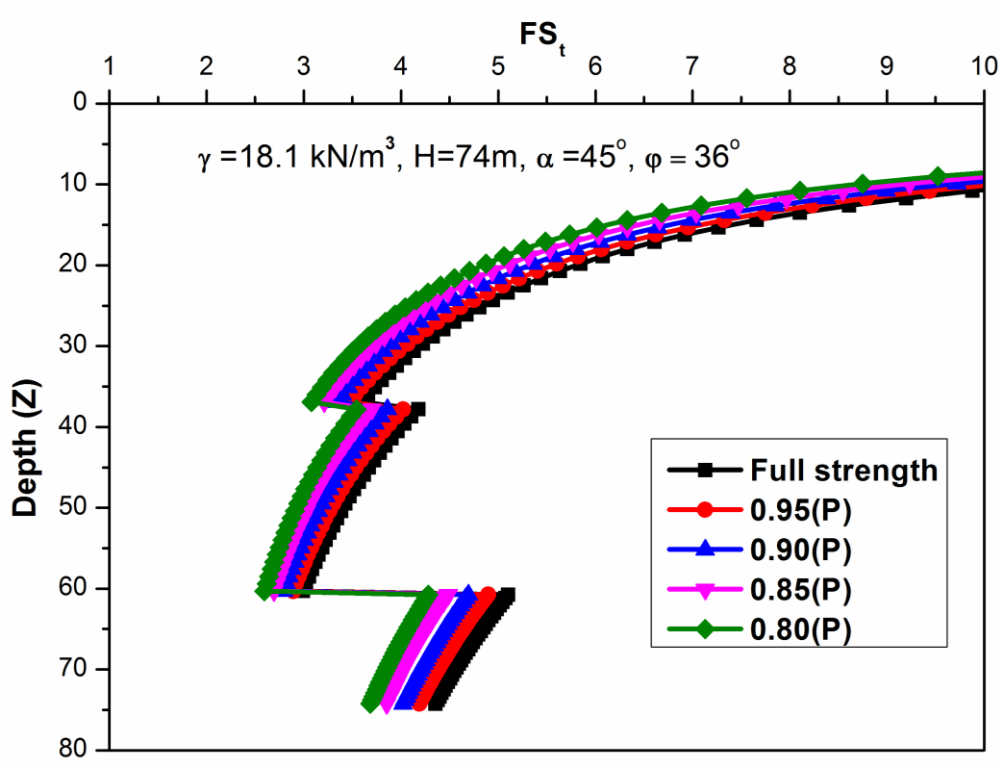

Figure 9. Factor of safety against tension for different values of reinforcement strengths

An important conclusion that can be made from this section that the reduction in friction angle from 36^o to 26^o could have made the GRS critical to tension and pullout failures. However, the failure images as shown in **Figs. 2, 3** and **4** do not show any signs of either overstressing or pullout failures. Therefore, a significant reduction in friction angle is highly unlikely.

Effect of Reduction in Design Strength of the Geogrids on Internal Stability

The reduced reinforcements strengths may be expected as there is a chance for the reinforcement to encounter the creep and biodegradation in the field. Therefore, results presented in **Fig. 9** shows the variation of a factor of safety against tension failure (FS_t) of 98 layers of reinforcement along the depth of wall for different reduced reinforcement strengths, $0.95\,T_{all}$, $0.9\,T_{all}$, $0.85\,T_{all}$ and $0.8\,T_{all}$ and typical values adopted in the above sections. It may be noted from **Fig. 9** that the bottom layers of reinforcement from the top of the wall are not critical to the tension mode of failure due to reduction in design strength of the reinforcement from 100 to 80%. Hence, the assumption of reduction in design strength of the reinforcement is not realistic.

Cause of the Collapse of Reinforced Soil Slope

Figs. 2 and **3** shows that the reinforced soil zone sheared where the reinforcement ended, and the reinforced soil as a whole is sliding down the hillside. The reinforcement is visible in the top layers, but not at the bottom. The fact is that it is at the base where the initial failure might have occurred, as this looks to be a rotational slide. The road embankment at the base of the slope as shown in **Fig. 3(a)** appears to be quite soft, with electricity poles leaning down the hill. Further,

it can also be noted that the area of bedrock exposure as shown in **Fig. 3(b)** shows flat lying sedimentary rock. It appears to include a competent pale sandstone over a greyish shale.

Another interesting observation that can be made from **Figs. 3(a)** and **3(b)** that the excavation and foundation of the GRS did not go to the base of the hill. The bedrock is visible in the back and presence of some moisture can be observed at somewhat higher in the slope. Lostumbo (2010) reported that foundation soil below the base of the GRS consists of "sandstone and some shale". The small intercalations of shale material can produce enormous bearing capacity problems. The low value of bearing capacity of shale can be attributed to lower compressive strength but more importantly significantly lower friction angle. Finally, an important conclusion that can be drawn from the study is that the founding bedrock failure is the most likely the cause of the collapse.

CONCLUSIONS

In an effort to recognize the potential causes of the failure of Yeager airport runway extension, the investigation is carried out for internal and external stability analysis. The findings of this forensic geotechnical investigation warrant the following conclusions.

1. It is observed that the considered long term design strength of the reinforcement and available length of the reinforcement are more than adequate to resist the tensile and pullout failure modes.
2. The failure cannot be attributed to either reduction in the friction angle due to improper compaction or reduction in the long term design strength of the reinforcement due to creep and biodegradation.
3. An important conclusion from the forensic investigation is that the founding bedrock failure is the most likely the cause of the collapse.

REFERENCES

Basha, B.M. & Babu, G.L.S. (2012). "Target reliability-based optimisation for internal seismic stability of reinforced soil structures." *Geotechnique,* No. 1, Vol. 62: 55–68.

FHWA (2001). *Mechanically stabilized earth walls and reinforced soil slopes: design and construction guidelines,* FHWA NHI-00- 43. Washington, DC: Federal Highway Administration and National Highway Institute.

Lostumbo, J.M. (2010). "Yeager Airport Runway Extension: Tallest Known 1H:1V Slope in U.S." *Proc. of GeoFlorida, 2010: Advances in Analysis, Modeling & Design,* GSP 199, 2010 ASCE.

Tencate, http://www.tencate.com/amer/Images/Reinforced%20Soil%20Case%20Studies_tcm29-19401.pdf